

(Dated: July 10, 2021)

Abstract

Valence band electronic structure of V_2O_3 : identification of V and O bands

E. Papalazarou,^{1,2,*} Matteo Gatti,^{3,4} M. Marsi,⁵ V. Brouet,⁵ F. Iori,^{3,4} Lucia Reining,^{3,4}
E. Annese,⁶ I. Vobornik,⁶ F. Offi,⁷ A. Fondacaro,⁸ S. Huotari,⁸ P. Lacovig,⁹
O. Tjernberg,^{8,10} N. B. Brookes,⁸ M. Sacchi,^{11,12} P. Metcalf,¹³ and G. Panaccione⁶

¹Laboratoire d'Optique Appliquée, ENSTA-Ecole Polytechnique, 91761 Palaiseau, France

²Laboratoire de Spectrométrie Ionique et Moléculaire,

Université Claude Bernard Lyon 1, 69622 Villeurbanne cedex, France

³Laboratoire des Solides Irradiés, Ecole Polytechnique, CNRS, CEA/DSM, 91128 Palaiseau, France

⁴European Theoretical Spectroscopy Facility (ETSF)

⁵Laboratoire de Physique des Solides, CNRS-UMR 8502, Université Paris-Sud, 91405 Orsay, France

⁶Laboratorio Nazionale TASC-INFN-CNR, in Area Science Park, I-34012 Trieste, Italy

⁷CNISM and Dipartimento di Fisica Università Roma Tre, I-00146 Roma, Italy

⁸European Synchrotron Radiation Facility, BP 220, F-38042 Grenoble Cedex 9, France

⁹Sincrotrone Trieste S.C.p.A., Strada Statale 14 km 163.5, I-34012 Trieste, Italy

¹⁰Materials Physics, Royal Institute of Technology KTH, Electrum 229, S-164 40 Kista, Sweden

¹¹Synchrotron SOLEIL, Boîte Postale 48, F-91142 Gif-sur-Yvette, France

¹²Laboratoire de Chimie Physique-Matière et Rayonnement,

Université Pierre et Marie Curie, UMR 7614, F-75005 Paris, France

¹³Department of Chemistry, Purdue University, West Lafayette, Indiana 47907, USA

(Dated: July 10, 2021)

We present a comprehensive study of the photon energy dependence of the valence band photoemission yield in the prototype Mott-Hubbard oxide V_2O_3 . The analysis of our experimental results, covering an extended photon energy range (20-6000 eV) and combined with GW calculations, allows us to identify the nature of the orbitals contributing to the total spectral weight at different binding energies, and in particular to locate the V 4s at about 8 eV binding energy. From this comparative analysis we can conclude that the intensity of the quasiparticle photoemission peak, observed close to the Fermi level in the paramagnetic metallic phase upon increasing photon energy, does not have a significant correlation with the intensity variation of the O 2p and V 3d yield, thus confirming that bulk sensitivity is an essential requirement for the detection of this coherent low energy excitation.

PACS numbers: 71.30.+h, 71.20.-b, 79.60.-i

The complex and fascinating physics of strongly correlated oxides has one of the most remarkable examples in vanadium sesquioxide, V_2O_3 , often considered as a prototype Mott-Hubbard system, where the competition between correlation and itinerant behavior of the electrons plays a crucial role in determining the electronic properties [1, 2]. V_2O_3 presents a rich phase diagram and undergoes, as a function of temperature, pressure and doping, a number of transitions passing from the paramagnetic metallic (PM) phase to the antiferromagnetic insulating (AFI) one, as well as from the PM to the paramagnetic insulator (PI) phase [3]. In the former case, the metal-insulator transition (MIT) is accompanied by a change of structure, from α -corundum to monoclinic, whereas the latter, obtained for instance by Cr doping, is isostructural.

In the description provided by dynamical mean-field theory (DMFT) [4], the coexistence of coherent quasiparticle (QP) features close to the Fermi energy E_F and incoherent lower Hubbard band (HB) at higher binding energy characterizes the correlated metallic phase of a Mott-Hubbard compound: V_2O_3 served as a test system to verify these predictions, and photoelectron spectroscopy (PES) played an important role to this end. In particular, high energy PES (using either soft or hard

X-rays) combining the direct probe of the electronic density of states (DOS) with enhanced bulk sensitivity [5], made it possible to reveal a clear coherent intensity near E_F [6, 7, 8]. Such a pronounced structure couldn't be observed in previous attempts using lower energy photons and a consequently more surface sensitive detection. Recent LDA+DMFT calculations [8, 9, 10] provide a good agreement with the experimentally determined shape and intensity for this peak, making it possible to extract quantitative information on fundamental physical parameters for a correlated systems, such as the effective Coulomb interaction parameter U .

Although a consensus has been reached for the presence of a QP intensity close to E_F in metallic V_2O_3 , several questions still remain unanswered, and call for a more detailed experimental and theoretical analysis of the V_2O_3 valence band, concerning in particular the role of the different V and O orbitals. On the experimental side, the difficulty in revealing the QP intensity has been mainly explained with the different electronic structure between surface and bulk. In general, not only the surface preparation of V_2O_3 may substantially alter the structural and electronic properties [11, 12], but also significant differences in QP intensity and lineshape could be found as a function of experimental conditions like for

instance the spot size of the probe [6]. This marked sensitivity to any perturbation of the bulk electronic structure has been recently interpreted as related to a surface dead layer where the QP vanishes, the essential physical reason being that the effects of the surface propagate over a characteristic length scale which is larger for strongly correlated materials [13, 14]. It is interesting to notice that the QP peak was found to give a prominent PES yield also when detected at very low (less than 10 eV) photon energy, where the level of bulk sensitivity of the photoelectrons increases again [13]. In fact, all these reports point out the importance of using bulk sensitive PES to obtain reliable information of QP intensity and transfer of spectral weight at MIT. At odd with this picture, cluster calculations on V_2O_3 suggest that the observed evolution of the QP spectral weight as a function of the photon energy should not be solely due to a change in surface vs bulk sensitivity, but that the change in V $3d/O$ $2p$ cross section ratio upon changing photon energy may also play an important role, given the V $3d-O$ $2p$ hybridization [15, 16]. Site specific PES experiments, together with density functional theory (DFT) calculations, investigated O-V hybridization: the theoretical analysis of the various contributions, together with fitted cross-sections and an approximate description of many body effects, could essentially reproduce the experimental spectrum taken at one specific photon energy ($h\nu=2286$ eV) [17].

The question of the interplay between hybridization and photon energy dependence of the spectra is hence one of the remaining key questions to be studied, in order to put the understanding of this complex material on a firmer basis. The prototype theoretical approach to the study of correlated materials, namely DMFT, suffers from the limitation that different kinds of orbitals are treated on different levels in order to keep the calculations feasible. Indeed, recent LDA+DMFT results for V_2O_3 [10] obtain that both the QP and the satellite are dominated by e_g^π states (while the a_{1g} has only a minor contribution), but the fact that these calculations treat p and d orbitals on a different footing doesn't allow one to draw definite conclusions about the hybridization. Methods that treat all orbitals on the same footing are typically band structure approaches like DFT in the Kohn-Sham (KS) formulation or approaches that describe band structure and additional features due to dynamical correlation (satellites) for situations where the band structure picture is still dominant. The state-of-the art approaches of the latter kind is the GW approximation, where the self-energy is calculated as a product of the one-electron Green's function G and the screened Coulomb interaction W [18]. Both the *ab initio* KS and the GW approaches are free of empirical parameters, which is a crucial point for our goal: hybridizations should be predicted, and then tested *a posteriori*, not simply fitted to experiment. Moreover, it is known that quasiparticle features calculated in GW are reliable even when satellites are not very

well described [19], so that the method can also be applied to transition metal oxides, as long as the question of interest is well defined in the quasiparticle framework.

We adopt hence in this work the KS and GW approaches for a theoretical description of the experimental spectra. GW is needed in order to obtain reliable positions of all quasiparticle features (including the O $2p$ and V $4s$ dominated region). We use a quasiparticle self-consistent GW approach where wavefunctions and energies are improved with respect to KS [20, 21]. It turns out that, close to the findings for similar materials [22], the change of wavefunctions with respect to a KS calculation mostly concerns a mixing between d states, whereas the $s-d$ and $p-d$ hybridization is already correctly predicted in KS-LDA. Concerning experiment, we present spectra consisting of extended valence band PES data from metallic stoichiometric V_2O_3 and Cr-doped $(V_{1-x}Cr_x)_2O_3$ ($x=0.11$), covering a very large range of photon energies, namely from $h\nu = 19$ to $h\nu = 5934$ eV. A large set of data is thus available for what concerns both intensity and lineshape variation of QP, along with a measurement of the entire V $3d$ and O $2p$ valence band region. The joint interpretation of calculated and measured spectra yields a coherent picture if the evolution of the structures close to the Fermi energy with increasing photon energy is attributed to surface effects, whereas the hypothesis of dominant $p-d$ mixing would not be consistent.

High quality single crystals, were grown at Purdue University using a skull melting technique [23] and characterized by XRD and SQUID measurements. PES experiments were performed using three different experimental setups: the VOLPE spectrometer for Hard x-ray PES [24] (ID16 beamline, base vacuum 9×10^{-10} mbar) and a Scienta SES-2002 for soft X-ray PES (ID08 beamline, base vacuum 1×10^{-10} mbar), both located at the European Synchrotron Radiation Facility (ESRF), and a Scienta SES-2002 for low energy PES (APE beamline, Elettra, Trieste - base vacuum 1×10^{-10} mbar). Spot size on the sample was $50 \times 120 \mu m^2$ and the overall energy resolution (beamline + analyser) was set to 450 meV (ID16 and ID08) and 50 meV (APE). The position of Fermi energy E_F and the overall energy resolution were estimated by measuring the metallic Fermi edge of polycrystalline Au foil in thermal and electric contact with the samples. The specimens were carefully aligned and fractured in UHV to expose the (0001) plane, and the photoelectrons were detected at normal emission. All the data presented here were taken at 200 K, which for $(V_{1-x}Cr_x)_2O_3$ corresponds to the PM phase both for $x=0$ and $x=0.11$, consistently giving identical results on several samples.

Figure 1 collects the extended valence band PES experimental spectra vs. photon energy. In each spectrum one recognizes two main spectral regions: one that we shall call VB, usually defined as the O $2p$ valence region, from 3 to 11 eV, and the other one between E_F

and 2-3 eV binding energy (BE), that we shall refer to as HB+QP. As the photon energy increases in the low photon energy range ($h\nu=19$ eV to 86 eV), the intensity of the HB+QP increases, relative to the one of the VB region. In agreement with previous experimental results [25], spectra in this photon energy range present a pronounced and broad feature, roughly centred at 6 eV BE, evolving in a clear three peaks structure when soft x-ray ($h\nu=700$ eV-900 eV) are used (see Fig. 2), with a residual tail of intensity at $BE > 10$ eV [6]. Interestingly, the spectral shape of the hard x-ray PES ($h\nu = 5934$ eV) spectrum is remarkably different, with a strongly dominant VB region extending down to $BE \sim 12$ eV, and a main peak at $\cong 8$ eV BE. A similar peak structure has also been observed in Hard X-ray valence band spectra of vanadates [26], cuprates [27] and manganites [28].

These results can be explained by the photon energy dependence of the cross sections of states with different symmetries as obtained in our calculations. In Fig. 2, indeed, the dotted, dot-dashed and dashed lines show the projection of the GW calculated density of states [36] on O $2p$, V $4s$ and V $3d$ contributions, respectively, multiplied by the Fermi distribution at 200 K. The contributions are then multiplied by a factor given by the corresponding change in cross section according to the used photon energy in the upper and lower panel, respectively, as taken from tabulated cross sections [33, 34] and shown in Table I [37]. We apply a Gaussian broadening of 0.4 eV simulating the experimental resolution. Moreover, since the incoherent part of the structure near the Fermi level is particularly strong as compared to the QP weight, in contrast to what one observes concerning the O $2p$ group, we add a Lorentzian broadening $\eta(BE) = 2.4 - 0.6BE$ for $BE < 4$ and thus simulate the redistribution of spectral weight that is not contained in our quasiparticle calculation. This procedure is justified if the HB and the QP are of same nature (i.e. V d in the present case), whereas in the case of strong $p-d$ hybridisation of the HB one should find a different result.

Although the only free parameter is the different broadening that we use for the QP+HB and the O $2p$ group, respectively, the good agreement with the experimental results is striking: not only is the qualitative behaviour nicely reproduced (e.g. the three-peak structure at 900 eV photon energy, evolving into a main peak with a low binding energy shoulder at 5934 eV), but also all absolute peak positions are in very good agreement with experimental structures [38]. This agreement allows us to draw unambiguous conclusions about the nature of the spectra. In particular, one can understand the strong peak that emerges at high photon energy at about 8 eV of binding energy as being entirely due to vanadium $4s$ states, and only to a minor extent to oxygen $2p$. The V $4s$ photoionisation cross section becomes dominant at high photon energy: as it can be seen from the table, cross section of O $2p$ and V $3d$ states in the range 200-

1400 eV are known to decrease in absolute value, while keeping almost constant their ratio [6, 33]

We now move to the inspection of the second region, HB+QP, by comparing selected experimental spectra in Fig. 3. As was evident from Fig. 1, a clear coherent intensity near E_F is observed at photon energies ≥ 700 eV. In this photon energy range the intensity ratio between the QP region and the HB one is almost constant, despite the big variation of intensity occurring in the VB region. In particular, the inset in Fig. 3 presents a zoom of the near E_F region, from $h\nu = 900$ eV and $h\nu = 5934$ eV PES spectra. The width of the QP and relative spectral weight of QP and HB are identical, within the noise level. Hence, the QP/HB ratio is not affected by the change of weight between Vs on one side and Op and Vd on the other side. On the contrary, the comparison between $h\nu = 900$ eV and $h\nu = 86$ eV spectra reveals that, although the QP intensity vanishes in the spectrum at $h\nu = 86$ eV, only minor spectral weight changes are observed in the VB region. Consider that, at this photon energy, most of the intensity in the VB has an O $2p$ character, due to cross section effects. Hence, if the change in the HB/QP ratio were dominated by O $2p$ hybridisation, one should have also observed major changes in the VB. Finally, when $h\nu = 86$ eV and $h\nu = 19$ eV are compared, QP+HB region results to be similar, whereas the intensity of VB region is highly enhanced at lower photon energy, which is again inconsistent with the hypothesis that O $2p$ plays a strong role in the HB.

The detailed variations within the low photon-energy range cannot be interpreted with tabulated cross sections; values are not available, and would moreover be hardly significant since at low energies, besides surface and many body effects, details of the density of empty states and material-specific matrix elements play a dominant role. In order to simulate these effects one should describe the photoelectron current J_E by

$$J_E(\omega) = \sum_{if} |M_{if}|^2 \delta(\epsilon_f - \epsilon_i - E) \delta(\epsilon_f - \omega). \quad (1)$$

In the one electron picture M_{if} are dipole matrix elements between occupied and empty one electron states of energy ϵ_i and ϵ_f , respectively, ω is the photoelectron energy and $E = h\nu$ is the photon energy. The common approximation to photoemission, namely the occupied DOS, is obtained when matrix elements M_{if} are kept constant and the second δ function (that represents energy conservation in the transition (i.e. a transition can only take place when final states in the reachable energetic region exist) is integrated over. In order to illustrate the qualitative importance of these contributions, we show in Fig. 4 the calculated spectra corresponding to 14, 37 and 50 eV of photon energy, respectively [39]. The continuous curve corresponds to Eq. (1), the dotted curve to the case where $M_{if} = const.$ is assumed. The dashed curve is the simple DOS, that does hence not

vary with photon energy. Strong effects of both contributions are found in this energy range on lineshape and intensity of the structures, and certain tendencies of the experiment can be detected (e.g. the fact that matrix elements tend to decrease the VB intensity with increasing photon energy). However, we stress the fact that agreement with experiment on this detailed level might be in part fortuitous, since our calculations do neither include surface effects nor the partial angle resolution that is instead present in experiment. These graphs are instead meant to illustrate the sensitivity of low-photon-energy spectra to both effects contained in our calculations, and not expected to be cancelled by the additional experimental features. They imply that one should be careful to interpret spectra based on symmetry analysis and hybridizations only.

Finally, only within the 0-2 eV region, theoretical and experimental results differ. Whereas the analysis based on the decomposition of the QP on the atomic angular momenta explains the main features in the VB region and their photon energy dependence, it does not predict the strong depletion of the quasiparticle peak at low photon energies in the HB+QP region, and also our calculations containing the bulk final state and matrix elements do not explain the disappearance of the QP at low photon energy. Indeed, as already pointed out, while the VB region is dominated by one-particle states, the region close to E_F is strongly influenced by incoherent structures due to strong correlation. Our results show that the measured spectra at $h\nu = 86$ eV and $h\nu = 37$ eV, while staying very similar in the 0-2 eV energy range, differ sizably in the VB region where O $2p$ contribution is dominant as shown in Fig. 3). This gives clear evidence against the hypothesis [16] that the particular evolution of HB+QP can be due to the fact that the HB has a relevant O $2p$ contribution while the QP is mainly V $3d$. Our results, based on an equal-footing treatment of p and d orbitals, and on experiment, suggest that both QP and HB are strongly V d -dominated, and give a comprehensive picture that is consistent with the hypothesis that QP and HB are influenced differently by the presence of the surface.

In conclusion, combining photoemission measurements performed at different photon energies with state-of-the-art GW calculations, we were able to disentangle the contribution of V $3d$, V $4s$ and O $2p$ orbitals to the valence band photoelectron yield of the prototype Mott compound V_2O_3 . Due to cross section effects, the V $4s$ band becomes particularly prominent in the hard X-ray regime, which makes it possible to unambiguously determine its binding energy at 8 eV from E_F . The possibility of including the orbitals of both V and O in ab initio calculations represents an important step forward towards a complete understanding of this model system, and allowed us to extract novel information on issues that are of general interest for many multi-orbital strongly correlated materials, like the level of hybridization between

different bands. For the specific case of V_2O_3 in its metallic phase, we were able to conclude that the QP peak and the lower HB have essentially a V $3d$ origin, and that the photon energy dependence of the QP/HB photoemission intensity cannot be explained only by O $2p$ /V $3d$ hybridization and cross section effects. These results confirm that bulk sensitivity is an essential requirement for photoemission studies of the electronic structure of correlated materials.

We acknowledge fruitful discussions with C. Giorgetti, P. Torelli, P. Wzietek and D. Jérôme. This work was supported by the 7th framework programme through the ETSF e-I3 infrastructure project (Grant agreement No. 211956), ANR project NT05-3 43900, the CEA nanoscience programme, and INFM-CNR. Work at Elettra was supported by the EEC through the initiative "Integrating Activity on Synchrotron and Free Electron Laser Science"

* Electronic address: evangelos.papalazarou@lasim.univ-lyon1.fr

- [1] N.F. Mott, *Metal-Insulator Transitions* (Taylor & Francis, London, 1990).
- [2] M. Imada *et al.*, Rev. Mod. Phys. **70**, 1039 (1998).
- [3] D. B. McWhan and J. P. Remeika, Phys. Rev. B **7**, 1920 (1973).
- [4] A. Georges *et al.*, Rev. Mod. Phys. **68**, 13 (1996).
- [5] A. Sekiyama *et al.*, Nature **403**, 396 (2000).
- [6] S.-K. Mo *et al.*, Phys. Rev. B **74**, 165101 (2006).
- [7] S.-K. Mo *et al.*, Phys. Rev. Lett. **90**, 186403 (2003).
- [8] G. Panaccione *et al.*, Phys. Rev. Lett. **97**, 116401 (2006).
- [9] G. Keller *et al.*, Phys. Rev. B **70**, 205116 (2004).
- [10] A. I. Poteryaev *et al.*, Phys. Rev. B **76**, 085127 (2007).
- [11] G. A. Thomas *et al.*, Phys. Rev. Lett. **73**, 1529 (1994).
- [12] D. S. Toledano *et al.*, Surf. Science **449**, 19 (2000).
- [13] F. Rodolakis *et al.*, Phys. Rev. Lett. **102**, 066805 (2009).
- [14] G. Borghi, M. Fabrizio, and E. Tosatti, Phys. Rev. Lett. **102**, 066806 (2009).
- [15] R. J. O. Mossaneck and M. Abbate, Phys Rev B **75**, 115110 (2007).
- [16] R. J. O. Mossaneck *et al.*, Phys. Rev. B **78**, 075103 (2008).
- [17] J. C. Woicik *et al.*, Phys. Rev. B **76**, 165101 (2007).
- [18] L. Hedin, Phys. Rev. **139**, A796 (1965).
- [19] F. Aryasetiawan and O. Gunnarsson, Rep. Prog. Phys. **61**, 237 (1998).
- [20] S. V. Faleev, M. van Schilfhaarde, and T. Kotani, Phys. Rev. Lett. **93**, 126406 (2004).
- [21] F. Bruneval, N. Vast, and L. Reining, Phys. Rev. B **74**, 045102 (2006).
- [22] M. Gatti *et al.*, Phys. Rev. Lett. **99**, 266402 (2008).
- [23] H. R. Harrison *et al.*, Mater. Res. Bull. **15**, 571 (1980).
- [24] P. Torelli *et al.*, Rev. Sci. Instr. **76**, 023909 (2005).
- [25] S. Shin *et al.*, Phys. Rev. B **41**, 4993 (1990).
- [26] R. Eguchi *et al.*, J. El. Spec. and Rel. Phenomena, **156** 421 (2007).
- [27] G. Panaccione *et al.*, Phys. Rev. B **77**, 125133 (2008).
- [28] F. Offi *et al.*, Phys. Rev. B **77**, 174422 (2008).
- [29] X. Gonze *et al.*, Comput. Mater. Sci. **25**, 478 (2002); X. Gonze *et al.*, Z. Kristallogr. **220**, 558 (2005);

<http://www.abinit.org>.

- [30] P.D. Dernier, J. Phys. Chem. Solids **31**, 2569 (1970).
- [31] N. Troullier and J. L. Martins, Phys. Rev. B **43**, 1993 (1991).
- [32] H. J. Monkhorst and J. D. Pack, Phys. Rev. B **13**, 5188 (1976).
- [33] J.J. Yeh and I. Lindau, Atomic Data and Nuclear Data Tables **32**, 1 (1985).
- [34] J. H. Scofield, Theoretical Photoionisation Cross Section from 1 to 1500 keV, LLNL Report UCRL-51326, 1973
- [35] V. Olevano *et al.*, <http://www.dp-code.org>.
- [36] We have used the ABINIT code for the ground state and GW calculations [29]. Calculations are performed at the experimental lattice parameters for pure V_2O_3 from [30]; we have checked that doping with Cr does not change significantly the DOS. We have employed Troullier-Martins pseudopotentials [31], including V $3s3p$ semicore states in valence. Convergence has been achieved with a $4 \times 4 \times 4$ Monkhorst-Pack [32] grid of \mathbf{k} points, an energy cutoff of 90 Ha in LDA and of 45 Ha for the wave functions entering the self-energy. In quasiparticle self-consistent GW calculations, where a plasmon-pole model has been adopted, all the states in the energy range from -10 to +5 eV have been calculated self-consistently.
- [37] For the spectrum at 5.934 KeV we have used the tabulated parameters at 6 KeV; for the spectrum at 900 eV we have taken an average of the values for 800 eV and 1000 eV.
- [38] GW corrections shift the LDA peak positions in the VB region by -0.7 eV on average. Of course the tabulated cross sections are a rather rough estimate and results could be further improved by fitting, but this is not the scope of the present work.
- [39] We have used the DP code [35] with 216 shifted \mathbf{k} -points.

TABLE I: Calculated V $3d$, V $4s$ and O $2p$ cross sections at selected photon energies, from Ref. [33] (a) and Ref. [34] (b). The values from Ref. [33], labeled 1 keV and 8 keV for simplicity, correspond to the tabulated values at 1041 eV and 8047.8 eV, respectively.

V and O cross sections at selected photon energies (Mbarns/electron)							
	21.2 eV	800 eV	1000 eV		6 keV	8 keV	
V $3d$	^a 1.94	^a 1.3×10^{-3}	^a 0.5×10^{-3}	^b 0.6×10^{-3}	^b 0.45×10^{-6}	^a 2×10^{-7}	^b 1.3×10^{-7}
V $4s$	^a 0.09	^a 9.5×10^{-4}	^a 0.5×10^{-3}	^b 0.6×10^{-3}	^b 1.2×10^{-5}	^a 5.5×10^{-6}	^b 5.9×10^{-6}
O $2p$	^a 2.6	^a 5.5×10^{-4}	^a 0.22×10^{-3}	^b 0.27×10^{-3}	^b 3.1×10^{-7}	^a 1×10^{-7}	^b 1×10^{-7}
Ratio $3d/4s$	21.5	1.37	1	1	0.038	0.036	0.022
Ratio $3d/2p$	0.75	2.36	2.27	2.22	1.45	2	1.3

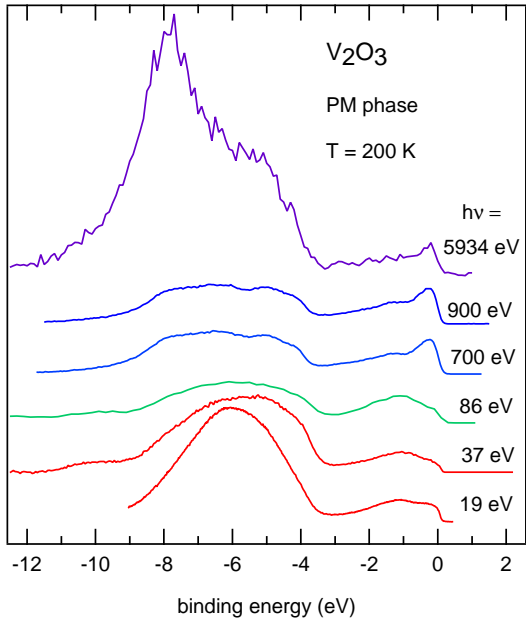


FIG. 1: (Color online) Experimental valence band PES spectra of V_2O_3 , normalized to the bottom of the incoherent spectral region at about -3 eV binding energy.

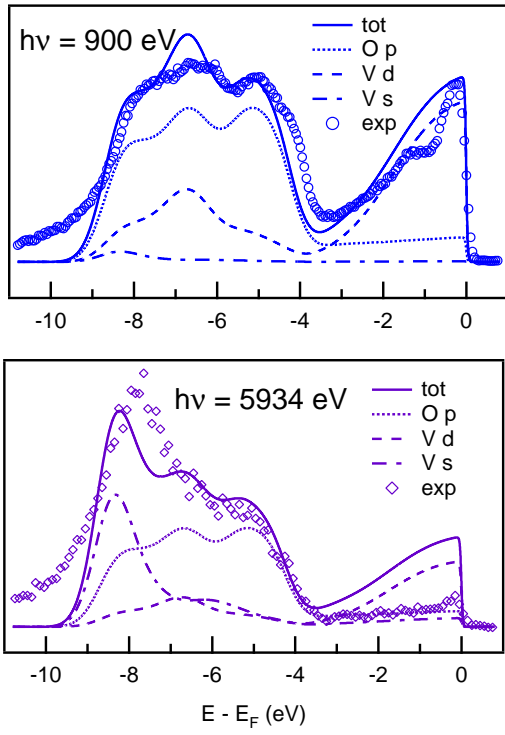


FIG. 2: (Color online) Measured valence band spectra compared to the total weighted DOS from GW calculations. The weighting has been obtained by multiplying partial s, p, d DOS's (see Table I).

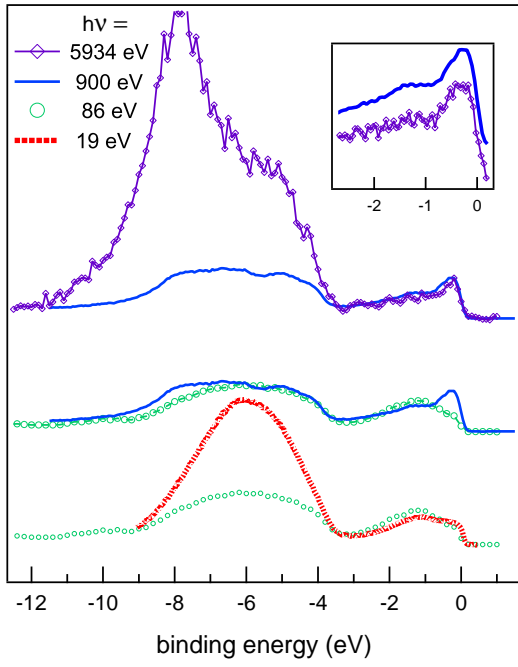


FIG. 3: (Color online) Direct comparison of selected pairs of experimental spectra taken at different photon energies. In the inset, the details of the QP region are shown for the two spectra at 900 and 5934 eV.

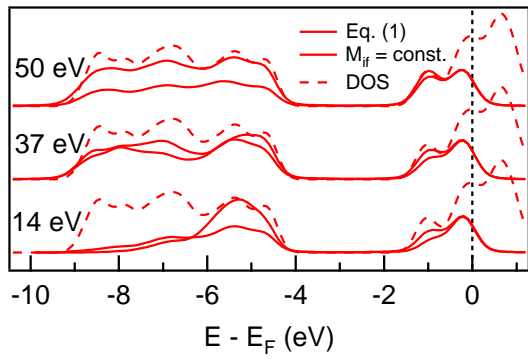


FIG. 4: Calculated spectra for different photon energies (14, 37 and 50 eV) using Eq. 1, including (continuous curves) or neglecting (dotted curves) matrix elements effects. The dashed curve (same for all photon energies) is the DOS.